

Coexisting oscillation modes and optical chaos in a hybrid ring cavity containing an induced absorber (CdS)

M. Wegener and C. Klingshirn

Physikalisches Institut der Universität, Robert-Mayer-Strasse 2-4, D-6000 Frankfurt am Main, Federal Republic of Germany

(Received 1 December 1986)

We investigate the self-oscillations of an induced absorber (CdS, photothermal effects) in a hybrid ring cavity. If the induced absorber is intrinsically bistable, we show that for a given set of system parameters different oscillation modes may exist depending on the initial conditions. In contrast to the behavior of an intrinsically bistable absorber, we find a bifurcation route to optical chaos if the induced absorber is not intrinsically bistable.

I. INTRODUCTION

In a recent paper¹ we have presented the first experimental investigation of the behavior of an induced absorber in a ring cavity. We use a hybrid ring cavity, which converts the intensity transmitted by the sample into a voltage signal which is delayed and fed back by use of an electro-optic modulator. The reader is referred to Ref. 1(a) for a description of the setup because we regard the present paper as an extension of Ref. 1(a). In Ref. 1(a) we characterized the optical bistability (OB) due to induced absorption, and showed how to measure the third normally unstable branch of the bistability with the help of the ring cavity. We also presented experimental evidence supporting the appearance of the Farey tree structure of oscillation periods as a function of the incident intensity predicted theoretically by Lindberg *et al.*,² and we discussed the dependence of the oscillations on various parameters. In this paper^{1(a)} we have concentrated on the behavior of an intrinsically bistable induced absorber in the ring cavity leading to the Farey tree structure in contrast to Ikeda instabilities,³ where generic routes to optical chaos do exist.

In the present paper we want to discuss further the properties of a ring cavity containing an induced absorber, which can only be described by taking into account that the system is infinite dimensional in the sense that an infinite number of initial conditions are necessary to describe the behavior.

In Sec. II we present the effect of mode coexistence both experimentally as well as theoretically for the case of an intrinsically bistable induced absorber. This effect has not been discussed in the theoretical papers.² We will show that in principle there exists an infinite set of coexisting modes.

Finally, in Sec. III a bifurcation route to chaos is observed in the case of a not-intrinsically-bistable absorber. This scenario is quite similar to Ikeda instabilities,³ which are also the product of a not-intrinsically-bistable nonlinear medium in the ring cavity.

II. THE EFFECT OF MODE COEXISTENCE

A. Experiment

In Fig. 1 we show three different measured oscillation modes for one fixed set of system parameters. The round

trip time τ_R is 500 ms which is roughly 500 times the relaxation time constant τ of the induced absorber and therefore large compared to τ . The polarization is $\mathbf{E} \parallel \mathbf{c}$ with \mathbf{c} being the crystallographic \mathbf{c} axis of the CdS single-crystal platelet at room temperature. The thickness L of the sample is $L = 3 \mu\text{m}$. The crystal shows intrinsic OB due to induced absorption under these conditions.

In agreement with Refs. 1 and 2 we denote a steplike oscillation where the transmitted intensity I_t rises for n round-trip times and decreases for m round trips as an (n, m) mode. The oscillation in Fig. 1(a) is denoted as a $(2, 1)$ mode. In Figs. 1(b) and 1(c) all system parameters as the reflectivity of the two semireflecting mirrors R and the incident intensity I_0 are kept constant. The only difference is that we have disturbed the system for a short time by putting a hand into the cavity. After a short transient phase one of the three oscillations in Fig. 1 is always obtained and remains stable. If I_0 is simply switched on and the system is left alone the oscillation in Fig. 1(a) always appears, and which we therefore call the basic mode. Only such modes are discussed in Refs. 1(a) and 2. A different way to excite one of the coexisting modes is to modulate the constant incident intensity for a short time. This is analogous to OB in that OB with two transmitted intensities exist when using I_0 as the control parameter, whereas in the present system multiple oscillation modes in the transmitted intensity exist when using the modulation of I_0 as the control parameter.

Looking at Figs. 1(b) and 1(c) or at Figs. 2(a) and 2(b), which show an enlarged view of the same measurements, one can see that in Figs. 1(b) and 1(c) one or two additional maxima per round-trip time are obtained, respectively. In the following we denote an oscillation as an $(n, m)_N$ mode when having N additional maxima per round trip compared to the basic $(n, m)_0 = (n, m)$ mode. In Figs. 2(a) and 2(b) it becomes obvious that the additional maxima always have the same structure as the basic mode, i.e., the plateaus of the steplike oscillations are situated at the same transmitted intensities. The oscillation $(2, 1)_1$ [Fig. 2(b)] is self-similar in that sense, because the twice-up—once-down structure is also present if one reduces the time scale to the order of the additional maximum.

The effect of mode coexistence is also observed for all other I_0 . Figure 2(c) shows one further example. I_0 is smaller as compared to Fig. 2(b) and therefore a $(4, 1)_2$

oscillation is obtained corresponding to the basic (4,1) mode. Again the additional maxima show the same structure as the basic mode. If τ_R is decreased we observe the coexisting modes disappear at about $\tau_R=200$ ms, while the basic modes vanish at about $\tau_R=2$ ms. [See Ref. 1(a).]

B. Theory

As discussed in Ref. 1(a) the whole system can be described by the two following equations:

$$I(t) = I_0 + R^2 I_t(t - \tau_R), \tag{1}$$

$$d(\Delta T)/dt = -\Delta T/\tau + A(\Delta T)I(t)/(CL), \tag{2}$$

with

$$A(\Delta T) = 1 - \exp[-\alpha(\Delta T)L],$$

$$I_t(t) = I(t) \exp[-\alpha(\Delta T(t))L],$$

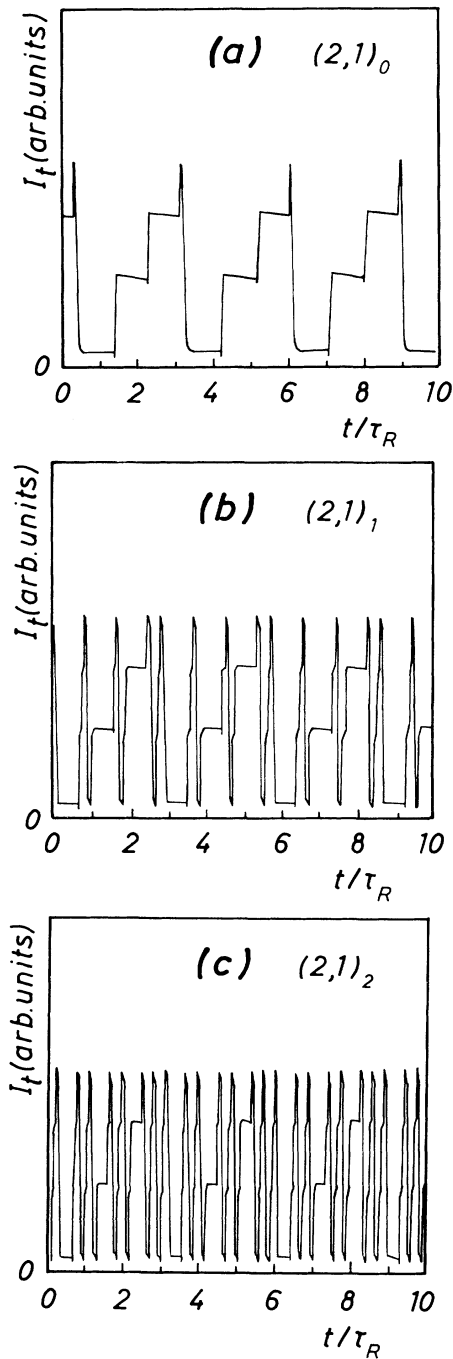


FIG. 1. Experimental appearance of coexisting modes for one fixed set of system parameters CdS, $\mathbf{E} \parallel \mathbf{c}$, $T=300$ K, $I_0=73\%$ I_1 , $R^2=75\%$, $\tau_R=500$ ms, $L=3$ μm , and $\hbar\omega=2.410$ eV.

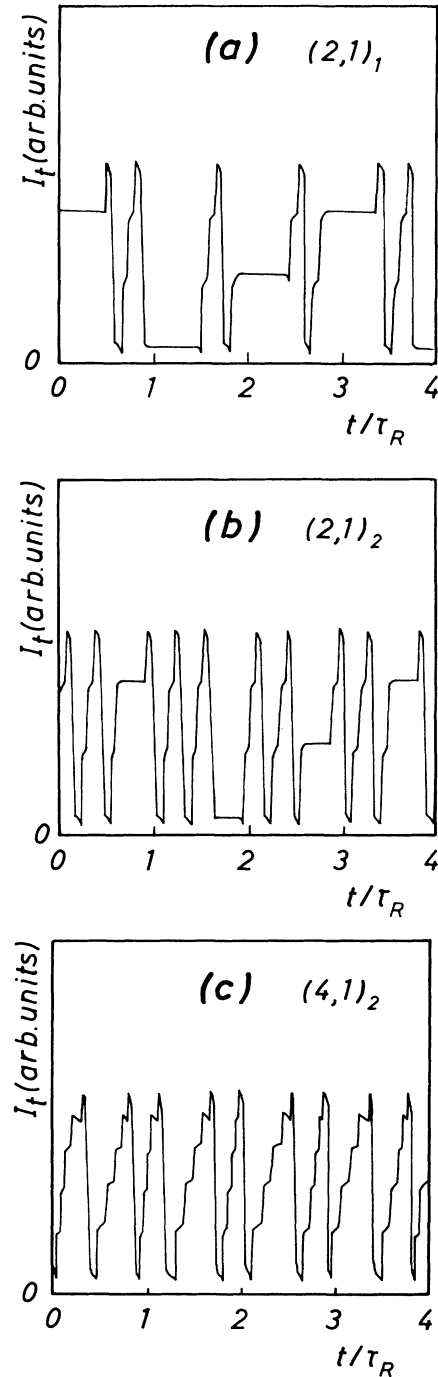


FIG. 2. (a) and (b) show the same measurement as Figs. 1(b) and 1(c) but on an enlarged scale. (c) is one coexisting oscillation to the (4,1) mode for $I_0=63\%$ I_1 .

and $\Delta T = T - T_0$ being the difference between the local temperature T in the laser spot and the surrounding heat bath T_0 , C the heat capacity, $I(t)$ the intensity in front of the crystal, and $\alpha(\Delta T)$ being the temperature-dependent absorption coefficient. In Eq. (1) we add intensities corresponding to our hybrid system [see Ref. 1(a)].

We want to start the discussion with the limit $\tau_R \gg \tau$. In this limit ΔT can be eliminated adiabatically. In order to simplify the situation further we use Eq. (1) and a schematic hysteresis Eq. (3):

$$I(t) = I_0 + R^2 I_t [I(t - \tau_R)], \quad (1')$$

$$I_t(I) = \begin{cases} I: & I < I_1 \text{ and higher branch,} \\ IT_L: & I > I_1 \text{ and lower branch,} \end{cases} \quad (3)$$

with T_L the transmission of the low transmitting branch. Note that $I_t(I)$ is bistable in the region $I_1 < I < I_1$.

In Fig. 3 we show three coexisting modes obtained with Eq. (3). In Fig. 3(a) the initial conditions are $I(t) = 0$, $0 < t < \tau_R$ obtaining the basic $(2,1)_0$ mode. In this case a reduction of the delay equation (1') to a one-dimensional mapping is possible, which is not the case in Figs. 3(b) and 3(c). Here one or two additional maxima, respectively, are taken into the initial state. Figure 3 corresponds closely to our experimental findings in Fig. 1. If additional maxima with a different position of the plateaus are chosen, the final state (when transients have died out) is always one of the types in Fig. 3.

In the present limit ($\tau_R \gg \tau$) an infinite number of coexisting modes exists, because the additional maxima can be made infinitely short with $N = 0, 1, \dots, \infty$. The frequency f of an $(n, m)_N$ oscillation is easily found to be

$$f((n, m)_N) = [1/(n + m) + N] \tau_R^{-1}, \quad (4)$$

demonstrating that the coexisting modes can be regarded as higher harmonics of the basic mode.

In order to be more realistic (τ_R/τ finite) we have to solve the coupled delay-differential Eqs. (1) and (2). As performed in Ref. 1(a) we use a fit to the measured $\alpha(\Delta T)$ (CdS, $\mathbf{E} \parallel \mathbf{c}$, $T_0 = 300$ K) for the numerical calculation. Now we are able to study the influence of a finite medium response time on the effect of mode coexistence.

Figure 4(a) again shows the simple $(2,1)$ oscillation for $\tau_R = 100\tau$ [see Fig. 16(a) in Ref. 1(a)]. Figure 4(b) presents the coexisting $(2,1)_1$ mode which is obtained after preparing the system in a state like Fig. 3(b). After a short transient phase the oscillations become periodic, oscillating with a higher frequency. Although the steplike structure is smeared out a little it can clearly be seen that the twice-up—once-down structure remains for $\tau_R = 100\tau$. The line in Fig. 4(a) has a length of $3\tau_R$ showing that the oscillation period has increased due to the finite medium response time. The period is increased a little further for the $(2,1)_1$ mode [in Fig. 4(b) the first line has a length of $3\tau_R$, the second line has a length of the $(2,1)_0$ period].

In Fig. 4(c) we have decreased τ_R by a factor of 10 to $\tau_R = 10\tau$. Under these conditions (the system is prepared into the same state as done for $\tau_R = 100\tau$ [Fig. 4(b)]) the coexisting mode is not stable and is damped out after a

short while. This fact is in good agreement with our experimental result, where we find no coexisting modes for $\tau_R < 200$ ms (see Sec. II A). For every finite τ_R/τ the number of coexisting modes (infinite for $\tau_R \gg \tau$) is reduced to a finite value and, e.g., in the experiment we never find more than three [$(2,1)_{N=0,1,2}$, $\tau_R = 500$ ms].

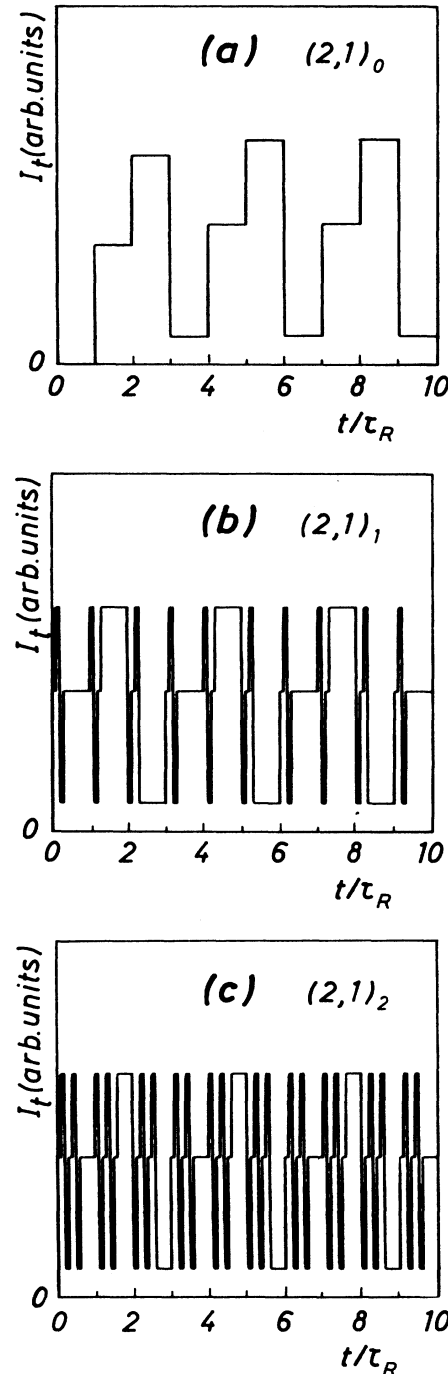


FIG. 3. Theoretical coexisting modes as obtained with Eq. (3), $T_L = 0.1$, $I_0 = 0.5 I_1$, $I_1 = 0.6 I_1$, and $R^2 = 75\%$. This series schematically describes our experimental findings in Fig. 1.

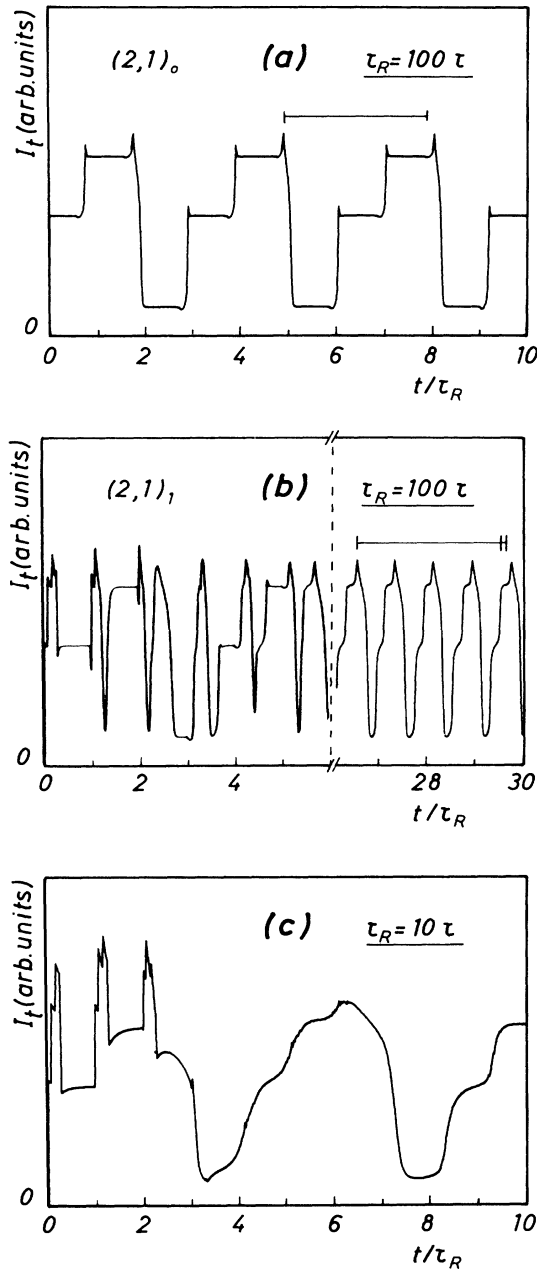


FIG. 4. Numerical solutions of Eqs. (1) and (2) showing that the coexisting $(2,1)_1$ mode is damped out for $\tau_R = 10\tau$. $R^2 = 1$, $\tau = 150 \mu\text{s}$, $I_0 = 130 \text{ Wcm}^{-2}$, and $L = 10 \mu\text{m}$.

III. THE RING CAVITY CONTAINING A NOT-INTRINSICALLY-BISTABLE ABSORBER

A. Experiment

In contrast to the behavior of an intrinsically bistable induced absorber (CdS, $\mathbf{E} \parallel \mathbf{c}$, $T_0 = 300 \text{ K}$, $\hbar\omega = 2.410 \text{ eV}$)

in the ring cavity, we find a bifurcation route to chaos if a not-intrinsically-bistable induced absorber (CdS, $\mathbf{E} \perp \mathbf{c}$, $T_0 = 300 \text{ K}$, $\hbar\omega = 2.410 \text{ eV}$) is taken.

In the polarization $\mathbf{E} \perp \mathbf{c}$ the medium is not bistable because the $A\Gamma_5$ exciton, which is dipole forbidden for $\mathbf{E} \parallel \mathbf{c}$, is allowed in the symmetry $\mathbf{E} \perp \mathbf{c}$. Therefore, the absorption edge is shifted into the fixed photon energy, the initial absorption $\alpha(\Delta T = 0)$ increases, and the slope of $\alpha(\Delta T)$ is not steep enough for the appearance of OB due to induced absorption. But the nonlinearity $\alpha(\Delta T)$ is still strong enough to obtain a regime with a steep negative slope of $I_t(I_0)$. This measured dependence is shown in Fig. 5 [the quadratic increase for small I_0 is explained in Ref. 1(a) and is the result of the fact that we do not measure I_0 with a separate photodiode but take the voltage signal applied to the Pockels cell modulating the incoming laser beam].

In Fig. 6 we present that we have measured for $I_t(t)$ when decreasing the constant incident intensity I_0 being in the limit $\tau_R \gg \tau$ ($\tau_R = 500 \text{ ms}$). For $I_0 = 93\% I_c$ [I_c is defined as the arithmetic average of the two extrema of the $I_t(I_0)$ curve shown in Fig. 5 and is therefore roughly situated in the middle of the steep negative slope of $I_t(I_0)$], a constant I_t corresponding to fixed points is observed. For $I_0 < 93\% I_c$, oscillations with a period of $2\tau_R$ appear. In Fig. 6(a) ($I_0 = 54\% I_c$) such an oscillation can be seen showing oscillations of higher frequency especially at the end of the steps. For $I_0 = 52\% I_c$ a bifurcation to period $4\tau_R$ is revealed. In Fig. 6(b) ($I_0 = 51\% I_c$) the difference to period $2\tau_R$ is much more pronounced. The amplitude of the additional high-frequency components has increased. Periods $8\tau_R$ or higher were not observed. For $I_0 < 50\% I_c$ we obtain oscillations which are irregular and are attributed to deterministic chaos. In Fig. 6(c) ($I_0 = 37\% I_c$, note the changed time scale) we show one example out of the chaotic regime, demonstrating that the locking into multiples of τ_R has totally vanished, the irregular structures are of the order of the previous high-frequency oscillations. We have analyzed the measured signal in Fig. 6(c) (using 600 data points) with the method

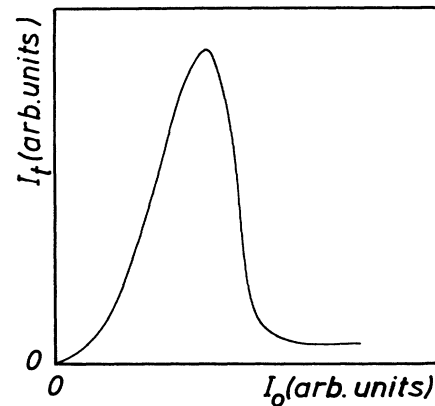


FIG. 5. I_t as a function of I_0 measured under the conditions CdS, $\mathbf{E} \perp \mathbf{c}$, $T_0 = 300 \text{ K}$, and $L = 3 \mu\text{m}$.

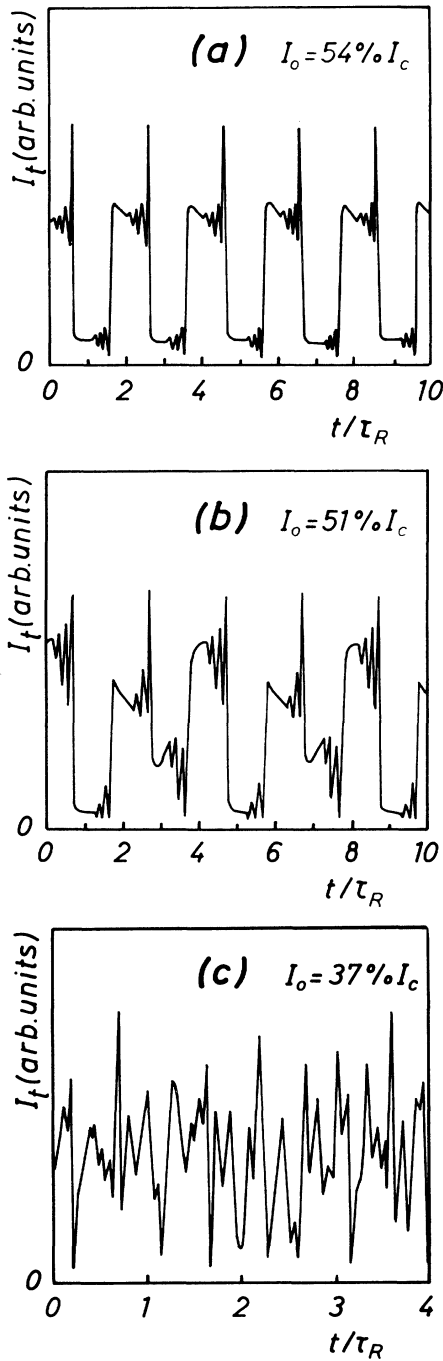


FIG. 6. Series of oscillations for decreasing I_0 using CdS, $E \perp c$, $T_0 = 300$ K, $L = 3 \mu\text{m}$, $R^2 = 1$, and $\tau_R = 500$ ms.

of Grassberger and Procaccia,^{4,5} briefly summarized in Eq. (5):

$$K_2 = \lim_{\substack{d \rightarrow \infty \\ l \rightarrow 0}} K_{2,d} \leq K, \\ K_{2,d} = \frac{1}{\tau_s} \ln[C_d(l)/C_{d+1}(l)], \quad (5)$$

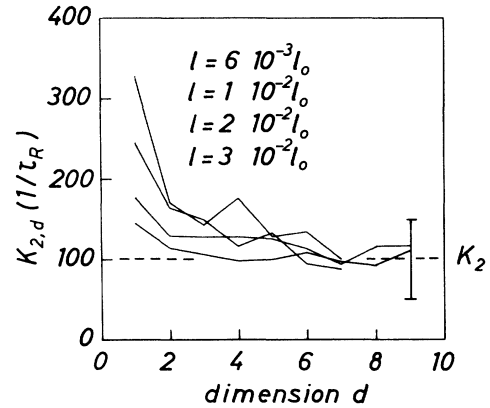


FIG. 7. $K_{2,d}$ as a function of the embedding dimension d , using the experimental data. The dependence is shown for various values of l .

$$C_d(l) = \lim_{N \rightarrow \infty} \frac{1}{N^2} \sum_{\substack{i,j=1 \\ (i \neq j)}}^N \Theta \left[l - \left(\sum_{k=1}^d (x_{i+k} - x_{j+k})^2 \right)^{1/2} \right],$$

$$x_i = I_t(i\tau_s).$$

K is the Kolmogorov entropy, K_2 is the correlation entropy, $C_d(l)$ is the correlation integral, d is the embedding dimension, and τ_s is the sampling time. For details see Ref. 5. A plot of $K_{2,d}$ is shown in Fig. 7, leading to the estimate of $K_2 = (100 \pm 50)\tau_R^{-1}$. This positive value confirms our interpretation of the irregular signal as deterministic chaos. The correlation dimension D_2 [which is the slope of $\ln(C_d)$ as a function of $\ln(l)$] is $D_2 = 2.6 \pm 0.3$.

B. Theory

Again we want to start the discussion with the so-called adiabatic limit $\tau_R \gg \tau$ which leads us to $d(\Delta T)/dt = 0$ in Eq. (2). Then ΔT can be expressed in terms of I and I_t only becomes a function of I . If we know the dependence $I_t(I)$ we can simply iterate Eq. (1').

In order to simplify things further we use a phenomenological ansatz for $I_t(I)$, which consists of two branches interpolated by a Fermi function:

$$I_t(I) = I \{ T_L + (1 - T_L) / \exp[S(I/I_c - 1)] + 1 \}$$

with $T_L = 0.05$, $S = 15$. The plotted dependence in Fig. 8(a) qualitatively describes the measured one in Fig. 5. In Fig. 8(b) we have iterated Eq. (1') with the $I_t(I)$ dependence in Fig. 8(a). This bifurcation diagram qualitatively fits our experimental findings as described in the experimental section. As is the case for all other maps following the Feigenbaum bifurcation scenario⁶ the sequence consists of an infinite number of period doublings. But as can be seen in Fig. 8(b) the range of period $8\tau_R$ is very small. If the noise level becomes comparable with the width of this range it is clear that the bifurcation will not

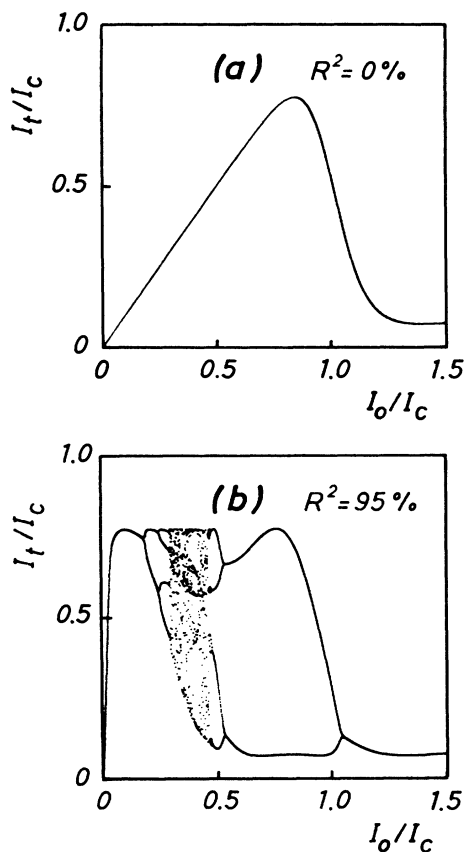


FIG. 8. (a) $R^2=0$ ($I_0=I$), corresponding to the nonlinearity of the medium itself. (b) $R^2=95\%$ shows the theoretical bifurcation diagram as obtain with the nonlinearity in (a).

be observable.

In a recent paper⁷ discussing Ikeda instabilities it was found numerically that the adiabatic limit is singular. When solving numerically a different set of delay-differential equations for a finite but great τ_R/τ they find

a finite number of bifurcations (with the parameters used only $2\tau_R$ and then chaos) although they have looked very carefully for further bifurcations. As is the case in our experiments they find high-frequency components in the $2\tau_R$ solutions and that the locking of the oscillations into multiples of τ_R disappears in the chaotic regime. They suggest the high-frequency oscillations are responsible for the termination of the period doubling sequence. It is hardly possible to decide experimentally whether the doubling sequence is finite or not because a certain noise level will always be present.

IV. CONCLUSION

In the present paper we have continued the discussion of the behavior of an intrinsically-bistable induced absorber (CdS) in a ring cavity^{1(a)} by presenting the effect of mode coexistence, which is a result of the infinite number of degrees of freedom of the system. Both experiments and theory are done here for the first time. The effect is analogous to optical bistability or multistability itself, respectively.

In contrast to the bistable absorber where a Farey tree structure of the oscillation period as a function of the incident intensity is found,^{2,1(a)} we find a bifurcation route to chaos if the absorber is not bistable. We show experimental indications that the adiabatic limit breaks down because of high-frequency components arising from the relaxation dynamics of the nonlinear medium.

ACKNOWLEDGMENTS

This work is a project of the Sonderforschungsbereich 65 "Festkörperspektroskopie" financed by the Deutsche Forschungsgemeinschaft. The high-quality CdS samples were grown in the Kristall-Labor der Universität Karlsruhe. Stimulating discussions with Dr. I. Galbraith and Professor Dr. H. Haug (Universität Frankfurt) are acknowledged. One of us (M.W.) would like to thank the Land Hessen for financial support.

^{1(a)} M. Wegener and C. Klingshirn, *Phys. Rev. A* **35**, 1740 (1987); (b) M. Wegener, C. Dörnfeld, M. Lambsdorff, F. Fidorra, and C. Klingshirn, *Proc. Soc. Photo-Opt. Instrum. Eng.* **667**, 102 (1986); (c) M. Wegener and C. Klingshirn, in *Proceedings of the Eighteenth International Conference on the Physics of Semiconductors* (World Scientific, Singapore, 1987), p. 1675.

^{2(a)} M. Lindberg, S. W. Koch, and H. Haug, *J. Opt. Soc. Am. B* **3**, 751 (1986); (b) in *Optical Bistability III, Proceedings of the Topical Meeting*, Vol. 8 of *Physics*, edited by H. M. Gibbs, P. Mandel, N. Peyghambarian, and S. D. Smith (Springer, Ber-

lin, 1986), p. 331; (c) H. Haug, S. W. Koch, and M. Lindberg, *Phys. Scr.* **34**, (1986).

³K. Ikeda, H. Daido, and O. Akimoto, *Phys. Rev. Lett.* **45**, 709 (1980).

⁴P. Grassberger and I. Procaccia, *Phys. Rev. Lett.* **50**, 346 (1983).

⁵P. Grassberger and I. Procaccia, *Phys. Rev. A* **28**, 2591 (1983).

⁶M. J. Feigenbaum, *J. Stat. Phys.* **19**, 25 (1978).

⁷M. Berre, F. Ressayre, A. Tallet, and H. M. Gibbs, *Phys. Rev. Lett.* **56**, 274 (1986).